Passive Inverted Ultra-Short Baseline Positioning for a Disc-Shaped Autonomous Underwater Vehicle: Design and Field Experiments

Yingqiang Wang, *Graduate Student Member, IEEE*, Ruoyu Hu, S. H. Huang, Zhikun Wang, Peizhou Du, Wencheng Yang, and Ying Chen

***Abstract*—Underwater positioning is critical to autonomous underwater vehicles (AUVs) for navigation and geo-referencing. The rapid attenuation of the electromagnetic wave in the underwater environment prevents the use of traditional positioning methods such as the Global Positioning System, whereupon acoustic methods like ultra-short baseline (USBL) positioning systems play an important role in AUV navigation. However, the high cost and complexity of classical USBL systems have stifled the democratization of these technologies, which leads to a new method called passive inverted ultra-short baseline (piUSBL) positioning. In a typical piUSBL system, a single beacon is placed at a reference point, periodically broadcasting a positioning signal. A passive USBL receiver, time-synchronized to the beacon, is mounted on an AUV to get one-way travel-time (OWTT) slant range and azimuth estimates. The passive nature of the receiver means the system is inexpensive, low-power, and lightweight. Particularly, the omnidirectional broadcasted signals offer a feasible solution for concurrent multi-AUV navigation. This letter demonstrates a full-stack design and development of a piUSBL positioning system, and presents evaluations of the accuracy and reliability of the system through a series of experiments. More significantly, a successful sea trial of a disc-shaped AUV outfitted with our piUSBL was conducted in the South China Sea.**

***Index Terms*—Marine robotics, localization, autonomous vehicle navigation.**

I. Introduction

AUTONOMOUS underwater vehicles (AUVs) have been increasingly used for a variety of applications in oceanographic science, offshore industry, and naval defense since their development in the 1970s [1], [2], [3]. Accurate and robust positioning in unstructured underwater environments is critical to AUVs for self-navigation, target tracking, or geo-referencing of scientific measurements. Conventional land positioning and navigation in fields are mainly based on the Global Positioning System (GPS), using radio-frequency communications which are however unavailable in underwater environments due to the rapid attenuation of electromagnetic waves. Therefore, underwater communications are generally acoustical-based, which is low-bandwidth and relatively unreliable, making navigation and localization in underwater environments particularly challenging [1], [3], [4], [5]. Current commercial AUVs typically use an inertial navigation system (INS), comprised of a Doppler velocity log (DVL) and a high-grade inertial measurement unit (IMU) with a fiber-optic or laser-ring gyroscope, to navigate through dead-reckoning between periodic GPS surface fixes for bounded error growth [6], [7], [8]. However, this classical method is bulky, power-hungry, and expensive, seriously restricting AUVs' popularity [8].

Underwater acoustic positioning, including long baseline (LBL), short baseline (SBL), and ultra-short baseline (USBL), can provide accurate coordinates for underwater applications without costly inertial sensors [1]. Particularly, USBL systems, composed of a single beacon and a transceiver with a hydrophone array, are widely used in AUV navigation for their portability and ease of use. In contrast, LBL and SBL systems are less used due to the time cost and expense of setting up the beacon network [9]. Conventional USBL systems determine the relative range and angle from the transceiver on the deployment ship to the beacon on the vehicle using two-way travel-time (TWTT) and phase differences. Problems exist with conventional USBL systems: TWTT measurements require AUVs to actively emit signals, which increases power consumption and decreases runtime; the request-and-response pattern is inefficient and complicated, reducing efficiency; if applied to multi-AUV systems, USBL systems should be assigned to different time slots or frequency bands to avoid interference, which is impractical for the underwater acoustic channel whose channel resource is rare [9].

A novel approach for underwater positioning, called passive inverted ultra-short baseline (piUSBL) positioning, has been developed in recent years and shows excellent feasibility and utility [4], [8], [9], [10], [11]. In piUSBL systems, a single acoustic beacon is placed on a deployment ship or a subsea station, periodically broadcasting an omnidirectional signal. A passive USBL receiver array that synchronously measures the positioning signal is mounted on the subsea AUV rather than the topside platform, explaining the so-called inverted mode. The relative range and angle between the single beacon and

Manuscript received December 1, 2021; accepted May 21, 2022. Date of publication May 27, 2022; date of current version June 9, 2022. This letter was recommended for publication by Associate Editor F. Zhang and Editor P. Pounds upon evaluation of the reviewers' comments. This work was supported by the National Key R&D Program of China under Grant 2017YFC0306100. *(Corresponding author: S. H. Huang.)*

The authors are with the Ocean College, Zhejiang University, Zhoushan 316021, China (e-mail: yingqiang_wang@zju.edu.cn; huruoyu@zju.edu.cn; davidhuang@zju.edu.cn; 11834011@zju.edu.cn; dpz@zju.edu.cn; wenc_yang@zju.edu.cn; ychen@zju.edu.cn).

Digital Object Identifier 10.1109/LRA.2022.3178494

TABLE I
TECHNICAL COMPARISON

Items	Zhejiang University (ZJU)	WHOI & MIT[7]
Core Architecture	FPGA (Timing, TX, RX) DSP (Signal processing)	Raspberry Pi 3
Circuit	Largely self-developed	Product-based
Clock	CSAC or OCXO[1]	CSAC
Array	Horizontal circular array	Tetrahedral array
Algorithm	Matched filter, CBF[2], dCv[3]	Matched filter and modified CBF
AUV platform	ZJU AUH	Bluefin SandShark
Effective range (reported)	> 1500 m	~ 500 m
Test depth (reported)	> 100 m	< 10 m

[1] Oven Controlled Crystal Oscillator.
[2] Conventional beamforming.
[3] Deconvolved conventional beamforming.

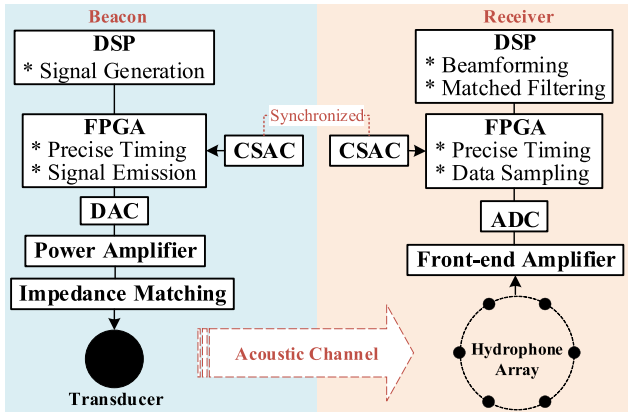

Fig. 1. System diagram of the piUSBL system. The acoustic beacon and receiver respectively transmit or record a predesigned acoustic signal when triggered by the PPS from the on-board CSAC which is disciplined to be aligned with the coordinated universal time from GPS. Acoustic measurements sensed by a hydrophone array are processed for range and angle estimation. Both ends are based on a dual-core architecture with a DSP and FPGA, completing signal generation, beamforming, matched filtering, adjustable gain control, precise timing, signal transmitting, and sampling.

the AUV are determined using one-way travel-time (OWTT) and phase differences, based on the synchronous clocks on both sides. Subsequently, the vehicle position is estimated through triangulation with the heading from an IMU [7], [8]. Thanks to the passive nature of the acoustic receiver, piUSBL systems help AUVs become low-cost, low-power, and lightweight. In particular, the omnidirectional signal from the beacon and the passive receiver of piUSBL makes it possible for multiple AUVs to self-locate and navigate concurrently and instantaneously, without sharing time slots or frequency bands which is inevitable for conventional USBL systems. Thus, the emergence of piUSBL enables AUV self-localization without relying upon expensive DVL-aided INS, which is of great significance to lower the threshold into marine robotics research or AUV-based scientific ocean observation. More importantly, piUSBL enables the ubiquitous and coordinated use of marine robots for the development of multi-AUV applications [7].

piUSBL has great potential in AUV navigation, but there are still few successful applications, most notably the work at the Woods Hole Oceanographic Institute (WHOI) and Massachusetts Institute of Technology (MIT), USA [7], [8], [9], [10]. The biggest difficulty preventing the development of the piUSBL technology is the lack of a small-size, low-power solution for accurate timing. It was only in recent years, when the first commercially available cesium-based chip-scale atomic clock (CSAC) was released by Microsemi, that the piUSBL technology began to become a reality [7]. Based on predecessors' work, this letter presents an independent full-stack work of a piUSBL positioning system for AUV navigation with new progress on some key issues, further demonstrating the feasibility and utility of piUSBL navigation for AUVs. The design and development of a piUSBL system are detailed from outside to inside. System calibration and essential evaluation were completed in an anechoic tank, showing the range and azimuth accuracy of $\mu \pm \sigma = 0.339 \pm 0.458^\circ$ and $\mu \pm \sigma = 0.023 \pm 0.035\,\mathrm{m}$ respectively in an ideal environment. Several field experiments in lakes and the sea also prove the accuracy and reliability of our piUSBL system, with a maximum effective range of over 1.5 km. Successful homing and docking guidance based on deployment of the piUSBL on a disc-shaped AUV is presented through field experiments.

Before going into the details, we brief the technical differences of ours (Zhejiang University) and that of WHOI & MIT, as presented in Table I.

The remainder of the paper is structured as follows. Section II describes the structure and principal components of this piUSBL system. Section III presents key methodologies of acoustic measurements, including matched filtering, array beamforming, and adjustable gain control. Section IV reports experimental results in an anechoic tank, field lakes, and the South China Sea. Section V summarizes the contributions and limitations of the current work and plans the future work.

II. STRUCTURE AND COMPONENTS

A. System Diagram

The piUSBL system consists of two basic components as outlined in Fig. 1: the acoustic beacon, which periodically broadcasts a predefined acoustic signal, and the passive USBL receiver, which synchronously measures and processes the target signal for the relative range and angle estimates between the beacon and receiver. A prominent characteristic of the piUSBL system is the time synchronization of the beacon and receiver, achieved by using two precise chip-scale atomic clocks (CSAC). Both ends consist of a digital signal processor (DSP) and a field-programmable gate array (FPGA) for rapid acoustic signal processing and precise underlying logic control. In brief, the system flow is as follows: the DSP in the acoustic beacon generates a user-defined acoustic signal, and then the FPGA transmits the signal when triggered by the rising edge of the pulse-per-second (PPS) from the CSAC; a digital-to-analog converter (DAC), a power amplifier and an impedance matching circuit converts the digital signal to a high-voltage analog signal with appropriate phase; the acoustic transducer therewith broadcasts the signal into the underwater acoustic channel; simultaneously, the FPGA in the receiver is triggered by the PPS from the

Fig. 2. *Left*: a commercial clock module with a Microchip Sa.45s CSAC. *Right*: a PPS disciplined oscillator module with an OCXO.

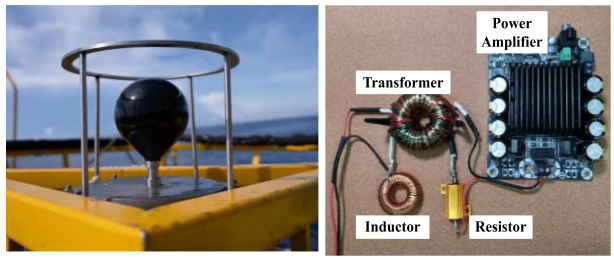

Fig. 3. *Left*: a spherical acoustic transducer mounted on the sealed cabin of the beacon. *Right*: the power amplifier and the impedance matching circuit which comprises a transformer, a resistor, and an inductor.

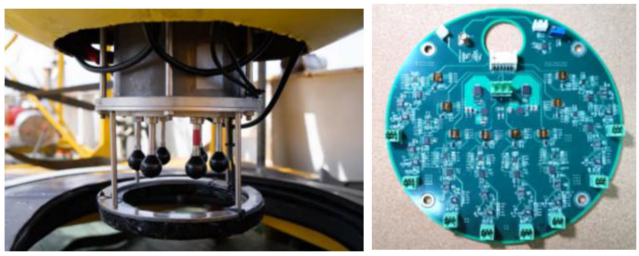

Fig. 4. *Left*: a 6-element hydrophone array on the acoustic receiver cabin mounted on the vehicle platform. *Right*: a self-developed 8-channel low-noise amplifier designed to amplify acoustic signal sensed by hydrophones, with two channels reserved for backup.

CSAC to collect acoustic data sensed by the hydrophone array using an analog-to-digital converter (ADC); digitized acoustic data are then processed onboard the DSP to obtain range and angle estimation through matched filtering and phased-array beamforming; finally, range and angle estimation is used by the vehicle for self-localization and navigation.

B. Accurate Timing

A prerequisite of an effective piUSBL system is accurate onboard timing on both the transmitting and receiving ends. As illustrated in Fig. 1, the two CSACs, fully disciplined before deployments to be aligned with the coordinated 1 PPS from GPS, provide accurate synchronized timing on both the beacon and receiver, enabling OWTT passive positioning. Consequently, timing error during the PPS-triggered transmitting and recording is considered a critical error source in OWTT ranging, which will directly reduce the accuracy of distance estimation.

The FPGA, which is used in both the acoustic beacon and the receiver, is a lynchpin component in our piUSBL system for accurate timing. FPGA-based programmable logics are utilized to increase the timing accuracy in signal transmitting and receiving. In comparison with software interrupt-based implementation, one may achieve the timing accuracy in the order of μs, which was in the order of ms reported in earlier implementation[7].

CSAC (Fig. 2, left) is an enabling technology for OWTT passive positioning, with characteristics of lightweight, low power consumption, and high accuracy (the drift is typically less than 100 μs/day) [7], [12]. Unfortunately, the fairly high price of CSAC (currently more than $4000 at retail) raises the cost of the piUSBL system, which is against our desire for a low-cost solution. An inexpensive choice – Oven Controlled Crystal Oscillator (OCXO, Fig. 2, right) is also an option to be considered with roughly one-tenth of the cost of CSAC, although OCXO drifts faster (roughly five times that of CSAC) and needs more power consumption [13]. In a previous evaluation that lasted 12 hours in the same environment, an OCXO drifted for 180 μs while the CSAC drifted for 40 μs – these delays at a sound velocity of 1500 m/s corresponds to 0.27 m and 0.06 m ranging errors respectively, which is acceptable in most short-term subsea applications.

C. Acoustic Beacon and Receiver

As illustrated in the left of Fig. 1, the acoustic beacon in our piUSBL system consists of seven main components. Except for the CSAC, DSP, FPGA, and DAC, we adopt an audio power amplifier, amplifying the waveform to a high-power signal. An impedance matching circuit is employed to match the impedance of the power amplifier and the transducer, which helps align the phase of voltage and current for maximum output power. A spherical transducer takes charge of transmitting the signal into the water uniformly in all directions, ensuring that any passive acoustic receiver within an effective distance can receive the valid signal. Thanks to the suitable transducer, amplifier, and impedance matching, as shown in Fig. 3, this acoustic beacon of our piUSBL provides an effective range of at least 1.5 km when broadcasts a signal with an appropriate frequency band.

The acoustic receiver of piUSBL (Fig.4, left) mainly accomplishes tasks as follows: passive sensing, signal amplification, analog-to-digital conversion, signal sampling, and onboard processing. A hydrophone array, a front-end amplifier, an analog-to-digital converter (ADC), a FPGA, and a DSP accomplish the tasks together, shown in the right of Fig. 1. To start sampling in sync with the broadcasts of the beacon, the passive receiver is triggered by the rising edge of the CSAC PPS that has been disciplined to be synchronized to the beacon CSAC before launch.

D. AUV Configuration

The piUSBL system is implemented on a disc-shaped AUV, also known as the autonomous underwater helicopter (AUH), as presented in Fig. 5. AUH is a new-invented member of the AUV family, designed to cruise near the sea bottom, land on and take-off from a subsea base station, executing tasks like in-situ observation, pipeline inspection, and target tracking[14], [15]. Equipped with a piUSBL receiver, the AUH can complete

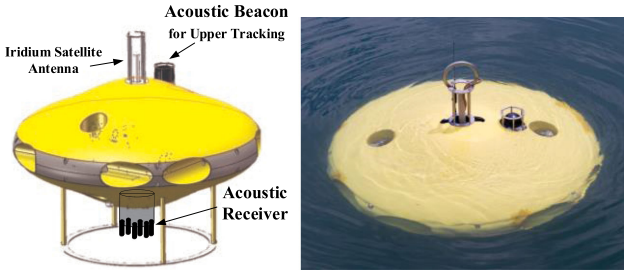

Fig. 5. *Left*: Diagram of the AUH carrying a piUSBL receiver, an Iridium satellite antenna, and an acoustic beacon for topside tracking. *Right*: Photography of an AUH on the surface of the Qiandao Lake.

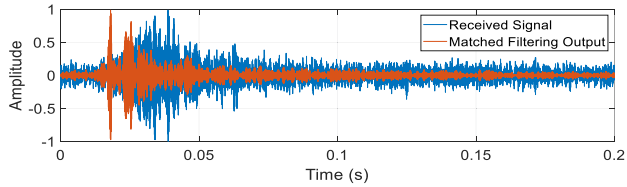

Fig. 6. A received signal in a field test and its matched filtering output. We can see a sharp crest that arises at the beginning of the valid signal, indicating the corresponding TOF. Thanks to the 20 ms, 10-12 kHz up-chirp, the matched filtering output owns a nice resolution.

self-localization and relative navigation when the acoustic beacon mounted on a subsea base station broadcasts the source signal. It is important to note that the acoustic beacon mounted on the top of the AUH is designed for topside tracking on the deployment ship, which is necessary for sea trials, rather than used for piUSBL positioning.

E. Array Geometry and Source Signal

Given that the AUH mainly executes tasks near the seabed while the acoustic beacon is also mounted on the subsea base station, horizontal azimuth is more critical to navigation because both the beacon and receiver are in an approximate horizontal near-bottom plane. We consequently designed a horizontal circular array with six elements uniformly distributed over the circumference with a radius of 0.065 m (Fig. 4, left), whose horizontal azimuth resolution is more excellent than vertical inclination resolution [7]. According to the half-wavelength theory, an operating frequency of 11.5 kHz at a sound velocity of 1500 m/s should be selected, as discussed below.

$$0.065\,m = \frac{1}{2}\cdot\lambda = \frac{1}{2}\cdot\frac{c}{f} \tag{1}$$

$$f = \frac{c}{0.13m} \approx 11.5kHz \tag{2}$$

In terms of better range resolution, we selected a 20 ms, 10-12 kHz linear frequency modulation (LFM) up-chirp as the source signal, which also suits the operating frequency of our acoustic transducer.

III. Acoustic Measurements

A. Matched Filtering

To estimate the range between the acoustic beacon and the receiver array, matched filtering is employed. Given the information of the positioning signal $x[n]$ broadcasted by the acoustic beacon, we use a matched filter to detect it within the signal $y_i[n]$ received by the *i*th hydrophone:

$$R_i[n] = \sum_{k=0}^{N-1} x[k]y_i[k+n], \tag{3}$$

where *N* is the discrete signal length of $x[n]$. The output $R_i[n]$ is maximum when $x[n]$ and $y_i[n]$ most closely match, indicating a one-way time of flight (TOF, also known as the time delay), shown in Fig. 6 with time as the X-axis. Because the origin of the circular array is exactly the horizontal center of the vehicle, we get the TOF *t* by averaging results of the six hydrophones:

$$t = \frac{1}{6f_s}\sum_{i=1}^{6}\arg\max_n(R_i[n]), \tag{4}$$

where f_s is defined as the sampling rate. Finally, the OWTT slant range is obtained by multiplying *t* and the local sound velocity, assuming that the signal travels along the direct path between the acoustic beacon and the piUSBL receiver. In a small localized area where the density of the water tends to be consistent, the local sound velocity can be derived by empirical formulas using conductivity, temperature, and depth. Considering more complex environments, a computational model of the acoustic channel is needed, with an accurate acoustic propagation profile [7].

B. Array Beamforming

To estimate the angle between the receiver and the beacon, which is a direction of arrival (DOA) estimation problem, we employed a conventional beamformer (CBF) (also known as a delay-and-sum beamformer). A typical CBF uses the array geometry and a hypothetical look-angle to apply time-delays to the signals received by the array, and sums the time-delayed signals for the output called beam power [9], [16]. When the given time-delays match the actual delays exactly, the hypothetical angle with the maximum CBF output is the likeliest DOA. Considering the array geometry and the principal mode of subsea horizontal movement of the AUH, we only do horizontal azimuth estimation to speed up onboard beamforming, where the CBF sweeps over a grid of look-angles from 0 to 360° in a given step length.

Given a horizontal circular array with *N* hydrophones uniformly distributed over the circumference with a radius of *R*, we can give the coordinates of the elements as

$$[x_n, y_n] = \left[R\cos\left(\frac{2\pi n}{N}\right), R\sin\left(\frac{2\pi n}{N}\right)\right], n = 1, 2, \ldots, N. \tag{5}$$

Assuming that a planar incident wave is from a source in the far-field and the hydrophone responses is isotropic, we can express the signals that arrive at an angle ϑ measured from the X-axis as $\mathbf{F} = \mathbf{A} * \mathbf{p} = [A_1p_1, A_2p_2, \ldots, A_3p_N]^T$, where $\mathbf{A} = [A_1, A_2, \ldots, A_N]^T$ is the amplitude and $\mathbf{p} = [p_1, p_2, \ldots, p_N]^T$ is the source-direction-dependent phase vector, defined by $p_n = \exp(-jk(x_n\cos\vartheta + y_n\sin\vartheta))$, in which $k = 2\pi/\lambda$ is the acoustic wave number and *j* is the imaginary number.

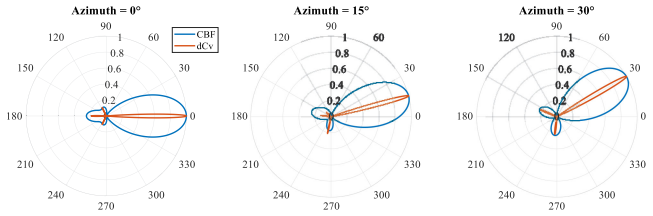

Fig. 7. Comparison plots of the CBF and dCv beam outputs in three different target angles. Both CBF and dCv perform well in detecting DOA, but the main beams of dCv are much narrower than that of CBF, as expected.

Before array beamforming, the signals received by the N hydrophones are normalized to $\mathbf{f} = \mathbf{p} = [p_1, p_2, \ldots, p_N]^T$, aiming to avoid errors caused by amplitude differences.

A steering vector derived by the array geometry and a hypothetical look-angle θ is $\mathbf{s} = [s_1, s_2, \ldots, s_N]^T$, defined by $s_n = (1/N)\exp(-jk(x_n \cos\theta + y_n \sin\theta))$. The phased-array beam output can be expressed as shown below[17], [18].

$$B(\theta) = \left|\mathbf{s}^H \mathbf{f}\right|^2 = \left| \frac{1}{N} \sum_{n=1}^{N} \exp\left\{ jk \left[x_n(\cos\theta - \cos\vartheta) + y_n(\sin\theta - \sin\vartheta) \right] \right\} \right|^2$$
$$= \left| \frac{1}{N} \sum_{n=1}^{N} \exp\left[j2kR \sin\left(\frac{\theta - \vartheta}{2}\right) \sin\left(\frac{2\pi n}{N} - \frac{\theta + \vartheta}{2}\right) \right] \right|^2 \tag{6}$$

As the primary method of DOA estimation, CBF is widely used for its robustness and simplicity, nevertheless suffers from fat beams and high-level sidelobes, which disturb maximum likelihood estimates [19]. It's undesirable for us to improve the performance of CBF by increasing the number of array elements which increases power consumption and system complexity. Therefore, we evaluated CBF and a new algorithm called deconvolved conventional beamforming (dCv) [16], [17]. Based on the determined beam pattern of the receiver array, the dCv algorithm deconvolves the CBF beam output to obtain narrower beamwidth and a lower sidelobe-to-peak ratio. As shown in Fig. 7, we employ CBF and dCv to detect three target azimuths, and obviously, dCv performs better than CBF. Nevertheless, the CBF algorithm is finally applied to the current embedded system because it is necessary to speed up the computation of dCv before its application, which demands more computational expense in the deconvolution process.

C. Adjustable Gain Control

Appropriate sensed signal strength, namely keeping the amplitude close to the ADC range, is essential for data sampling when the signal strength changes with the distance between the beacon and the piUSBL receiver. We address this by introducing an adjustable gain control (AGC) process that keeps evaluating the power of target signals and timely adjusts the receive gain to maintain a reasonable ADC-input signal amplitude. The receive gain corresponds to a variable voltage that controls a voltage-controlled amplifier (VCA) on the front-end amplifier board (Fig. 4, right).

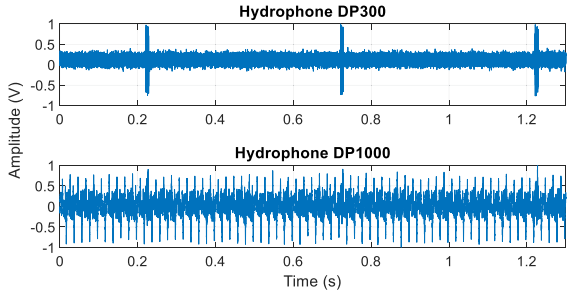

Fig. 8. An evaluation of two models of hydrophones, DP300 and DP1000. The hydrophones were placed at the same position and a depth of 2 m, using the same front-end amplifier. A beacon was deployed to broadcast an extremely weak signal at a rate of 2 Hz. It's easy to tell the DP300 performing better.

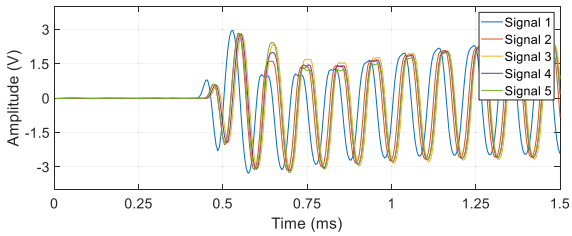

Fig. 9. The measurement of system delay by recording the acoustic signal with the beacon placed next to the hydrophone array presupposing a distance of zero. The 0.5 ms delay at a sound velocity of 1500 m/s corresponds to a 0.75 m error.

IV. Experimental Results

A. System Calibration

To evaluate and improve the accuracy and maximum effective range, we performed experiments in a 50 m $*$ 15 m $*$ 10 m anechoic tank whose acoustic environment is ideal for system calibration. The selection of hydrophones with proper acousto-electric conversion performance is essential for extending the effective range. We evaluated two models of hydrophones using the same amplifier and an extremely weak signal broadcasted by our beacon, which helps us choose the DP300 for the following works, shown in Fig. 8.

As mentioned in the section of accurate timing, the broadcast and recording are both triggered by the PPS from the synchronized CSACs, achieving a theoretically perfect synchronization. However, in practical situations, the system delay caused by analog filtering, data sampling, and clock drifting will be wrongly counted into the TOF for range estimation [12]. Thanks to the use of FPGA for timing and sampling, the system delay of our piUSBL mainly comes from analog processes, which is pretty steady at about 0.5 ms, as illustrated in Fig. 9. In practice, we subtract the characterized system delay in distance estimation.

To have an understanding of the accuracy of the piUSBL system, we subsequently performed comparison experiments between our piUSBL and the servo system with reliable angle and distance reference above the anechoic tank. Our acoustic beacon was submerged to 4 m depth and fastened at a known position according to the ruler along the tank. The piUSBL receiver was placed at the same depth but rigidly connected to the servo system for rotation and horizontal movements.

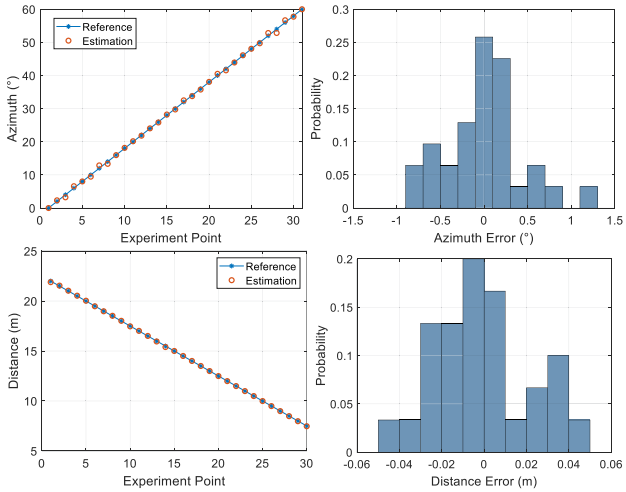

Fig. 10. *Left*: Azimuth and range estimates between the beacon and receiver array in orange, with true azimuth and distance reference from the readings of the servo system in blue. *Right*: Histograms of error distribution of the raw acoustic measurements.

Comparison plots of azimuth and distance between the piUSBL system estimates and the servo system reference can be seen in the left of Fig. 10, which demonstrate good agreement. The histograms of error distribution are illustrated in the right of Fig. 10, indicating that this piUSBL system can provide raw acoustic measurement accuracies of $\mu \pm \sigma = 0.339 \pm 0.458°$ and $\mu \pm \sigma = 0.023 \pm 0.035\,\mathrm{m}$ in azimuth and range respectively, while μ and σ represent mean and standard deviations. The azimuth errors are likely due to acoustic reflection between the hydrophones and local acoustic effects with the mounting surface of the receiver array, where the mean deviation of 0.339° may be caused by the initial installation error between our array and the servo system. Meanwhile, the relatively small distance errors may come from the stochastic error of the piUSBL system and the kinematic error of the servo system.

B. Lake Experiments

Field experiments were carried out in a 300 m $*$ 200 m $*$ 5 m lake named Tannong Reservoir near our campus to uncover more potential problems in actual environments. After several failures and system adjustments, we conducted a successful field lake experiment, as illustrated in Fig. 11. The acoustic beacon was mounted on the yellow tripod and submerged to the lakebed at about 5 m depth. A differential GPS (DGPS), whose positioning and heading accuracy is within 10 cm and 0.5° with a 2 m baseline of antennas, provides an accurate ground-truth comparison for the acoustic estimates when rigidly connected to the piUSBL receiver.

In the azimuth estimation test, we rotated the frame attached to the piUSBL receiver and recorded the acoustic estimates and DGPS heading reference, with the comparison plots and the error statistics shown at the top of Fig. 12. The azimuth accuracy of $\mu \pm \sigma = 1.909 \pm 2.375°$ is worse than that of tank experiments, which is thought to be the result of the non-perfect rigid attachment of the receiver to the aluminum frame, and complex field acoustic effects such as multipath and reflections.

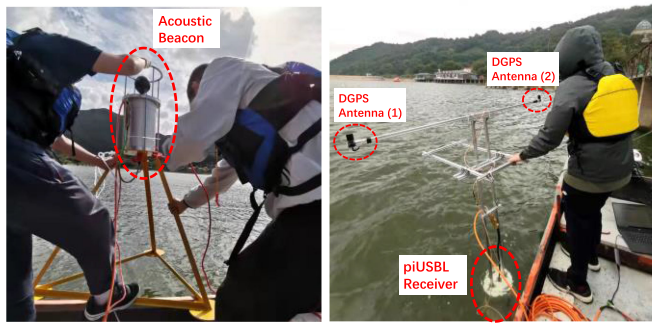

Fig. 11. Setup of the lake experiments in Tannong Reservoir. *Left*: The acoustic beacon was mounted on a tripod and submerged to the lakebed. *Right*: The piUSBL receiver array was rigidly connected to a DGPS receiver for ground-truth reference.

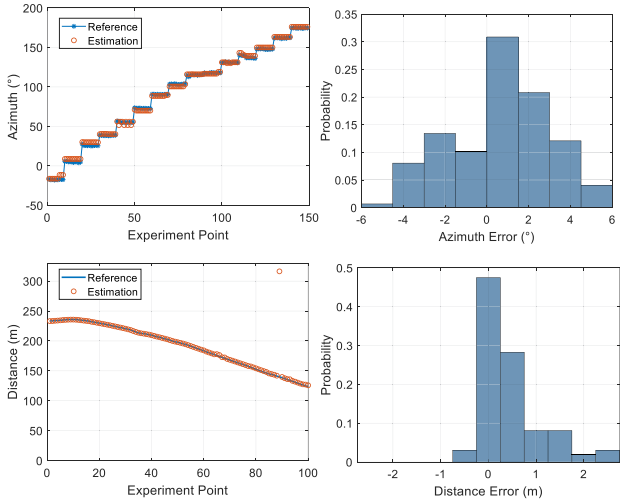

Fig. 12. *Left*: Azimuth and range estimates between the beacon and receiver in orange, with ground-truth reference from DGPS in blue. *Right*: Histograms of error distribution of the raw acoustic measurements, with the outlier of distance estimation removed.

The distance estimation test was performed by moving the receiver using a surface boat, similarly keeping the array underwater and the DGPS in the air. An obvious outlier at the end of the experiment, shown in the bottom left of Fig. 12, comes from an accidental timing failure due to an FPGA bug. The error distribution indicates the distance estimation accuracy of $\mu \pm \sigma = 0.475 \pm 0.638\,\mathrm{m}$, while the errors may come from the sway and horizontal drift of the surface boat between data sampling and fetching the DGPS information.

After experiments in the Tannong Reservoir, we performed another field experiment with an AUV in the Qiandao Lake, an artificial reservoir that is much bigger and deeper. In this experiment, our piUSBL receiver was mounted on a disc-shaped AUV, which is named G-AUH and equipped with a micro-electro-mechanical-system (MEMS) inertial measurement unit (IMU) (with a magnetometer) for an estimate of vehicle attitude and heading, shown in the right of Fig. 5. The acoustic beacon was fixed in the lakebed at about 60 m depth. As illustrated in the upside of Fig. 13, the G-AUH outfitted with the receiver moved away from the beacon and returned after a set time, then moved

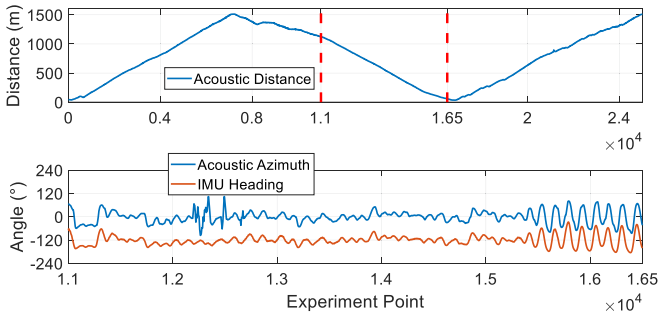

Fig. 13. *Upside*: Acoustic estimates of the distance between the acoustic beacon and the G-AUH in the Qiandao Lake. *Downside*: Comparison plots of the acoustic azimuth estimates and the IMU heading, and the range of the X-axis is indicated by the red dotted lines in the upside figure. Some non-ideal local lakebed topography may cause the outliers in the acoustic azimuth. Note that the estimates have been smoothed using moving average.

Fig. 14. Photograph of the G-AUH (*left*) and the subsea base station (*right*) to be deployed into the sea, taken on the R/V *YueZhanYuKe-3* during the cruise in September 2021. Our piUSBL receiver and the acoustic beacon are respectively mounted on the G-AUH and the subsea base station.

away again, with a maximum distance between the vehicle and beacon over 1.5 km, as recorded by the piUSBL system. It is worth noting that the process of returning was under the guidance of our piUSBL system by keeping the acoustic azimuth equal to zero, given that the zero orientation of the receiver array was aligned with the bow of the G-AUH. The IMU heading estimated by the magnetometer is an absolute angle relative to the north, while the acoustic azimuth is a relative angle between the receiver array and the beacon, which means the two angles are independent but should show a similar trend of change during the process of returning.

Comparison plots of the acoustic azimuth and the IMU heading during the returning are presented in the downside of Fig. 13, where two lines show a consistent trend of change despite some outliers of acoustic measurements, with the piUSBL azimuth estimates oscillating around zero, indicating that our piUSBL provided a reliable estimate of azimuth.

C. Sea Trial

To verify the actual performance of the piUSBL positioning system, sea experiments were carried out in September 2021 in the South China Sea, using our piUSBL positioning system and the G-AUH. The piUSBL receiver was installed under the G-AUH, and the acoustic beacon was mounted on the subsea base station, as shown in Fig. 14.

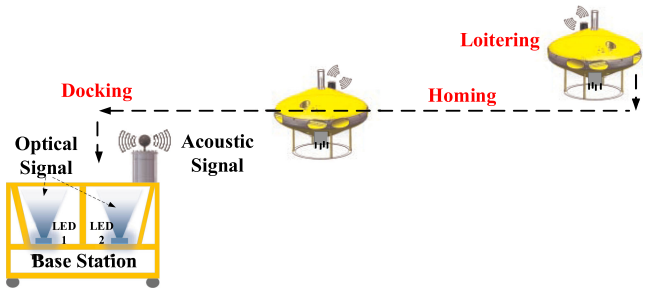

Fig. 15. The procedure of the sea experiment conducted in the South China Sea, which is designed to examine the actual performance of the G-AUH and our piUSBL positioning system.

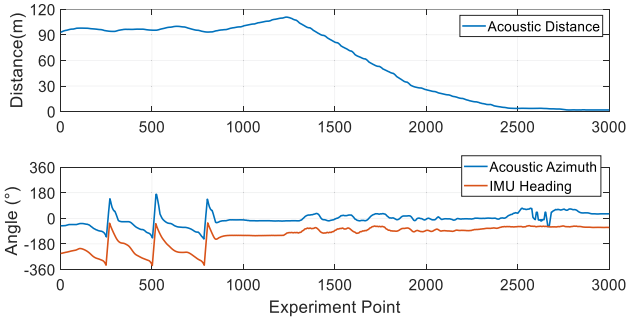

Fig. 16. *Upside*: Acoustic estimates of the distance between the acoustic beacon and the G-AUH in the South China Sea. *Downside*: Comparison plots of the acoustic azimuth estimates and the IMU heading. The outliers of the acoustic azimuth may come from the influence of seabed topography and the propeller noise of the G-AUH. The estimates have been smoothed using moving average.

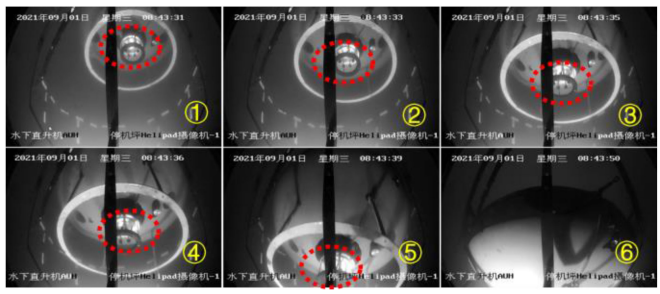

Fig. 17. Photograph of the optically guided docking process of the G-AUH in the South China Sea experiment, recorded by a camera on the subsea base station. The yellow numbers indicate the order of images, and our piUSBL receiver is marked by the red dotted lines.

The procedure of the sea experiment is illustrated in Fig. 15: firstly, the subsea base station, equipped with our acoustic beacon and two blue LED lights, was submerged to the sea bottom at 102 m depth, as shown in the right of Fig. 14; secondly, the G-AUH outfitted with our piUSBL receiver was deployed about 100 m away from the beacon and started diving to a depth of about 92 m; thirdly, when the beacon started broadcasting the positioning signal, the G-AUH loitered for a while to get stable acoustic measurements and subsequently began to home-in on the subsea base station under the guidance of the relative position of the piUSBL system; finally, the G-AUH completed docking into the base station with the help of optical guidance using a vehicle-equipped camera and the LED lights on the station.

The movement of loitering and homing is clearly illustrated in Fig. 16. In the loitering period, the acoustic distance slowly

varies between 90 and 110 m, and the acoustic azimuth and IMU heading indicate three horizontal rotations, which means the G-AUH is searching for the acoustic azimuth of zero before homing. After the G-AUH locks on the target azimuth of zero, it starts to home-in on the acoustic beacon, as presented by the decreasing acoustic distance and the corresponding acoustic azimuth near zero, shown in Fig. 16.

Once the piUSBL system has successfully guided the G-AUH to within 20 m of the base station, the camera on the vehicle is activated to search for the LED lights, and the G-AUH will complete docking into the subsea base station under the optical guidance, shown in Fig. 17.

V. Conclusion

This work has completed a full-stack design and development of a passive inverted ultra-short baseline (piUSBL) positioning system for AUV navigation and experimentally evaluated the accuracy and reliability of the system through a series of tank and field experiments. The piUSBL system uses an acoustic beacon to broadcast a predesigned signal, and an AUV-mounted receiver array, which is time-synchronized to the beacon, to passively estimate OWTT slant range and relative azimuth between the receiver array and beacon using matched filtering and array beamforming. The use of a single beacon and the passive receiver makes the piUSBL system low-cost, low-power, and easy to deploy. More than that, the omnidirectional signal from the beacon and the passive nature of the piUSBL receiver means that a multitude of AUVs can concurrently use the piUSBL system to self-locate and navigate.

The evaluation experiments of the piUSBL system in the anechoic tank demonstrate the acoustic range and azimuth measurement accuracies of about $\mu \pm \sigma = 0.339 \pm 0.458^\circ$ and $\mu \pm \sigma = 0.023 \pm 0.035\,\mathrm{m}$ respectively. In the comparison experiments between the piUSBL system and a DGPS in the Tannong Reservoir, the acoustic system can provide raw measurement accuracies of $\mu \pm \sigma = 1.909 \pm 2.375^\circ$ and $\mu \pm \sigma = 0.475 \pm 0.638\,\mathrm{m}$ in azimuth and range respectively. Subsequent experiments in the Qiandao Lake and the South China Sea indicate that our system can provide a maximum effective range over 1.5 km and reliable acoustic estimates to the AUV for homing guidance in field environments.

A number of limitations still exist in the current form of our piUSBL system: firstly, we have only performed relative navigation between the acoustic receiver and beacon because absolute navigation requires IMU heading estimates, but the heading accuracy of MEMS IMU is relatively poor; secondly, complex acoustic effects such as multipath and reflections in the field will reduce our positioning accuracy; thirdly, the piUSBL receiver mounted on an AUV is susceptible to the propeller noise which reduces the signal-to-noise ratio (SNR).

Future work includes simultaneously deploying multiple beacons to combine long baseline (LBL) and piUSBL positioning systems, which can help AUVs get absolute position and heading by acoustic measurements; further research on the deconvolved conventional beamforming for high-resolution multi-target DOA estimation in the combined system of LBL and piUSBL; and research on adaptive noise cancellation for improving the performance of the passive acoustic receiver; and further study on applying the piUSBL to multi-AUV systems.

Acknowledgment

The authors would like to thank the AUH research team at Zhejiang University, Shenyang Institute of Automation at Chinese Academy of Sciences (CAS), and Institute of Deep-sea Science and Engineering at CAS for experiment support. They also thank all the crew members of the R/V *YueZhanYuKe-3* for their cooperation during the cruise.

References

[1] L. Paull, S. Saeedi, M. Seto, and H. Li, "AUV navigation and localization: A review," *IEEE J. Ocean. Eng.*, vol. 39, no. 1, pp. 131–149, Jan. 2014.

[2] E. M. Fischell, A. R. Kroo, and B. W. O'Neill, "Single-Hydrophone low-cost underwater vehicle swarming," *IEEE Robot. Automat. Lett.*, vol. 5, no. 2, pp. 354–361, Apr. 2020.

[3] J. Kim, "Cooperative localization and unknown currents estimation using multiple autonomous underwater vehicles," *IEEE Robot. Automat. Lett.*, vol. 5, no. 2, pp. 2365–2371, Apr. 2020.

[4] E. M. Fischell, N. R. Rypkema, and H. Schmidt, "Relative autonomy and navigation for command and control of low-cost autonomous underwater vehicles," *IEEE Robot. Automat. Lett.*, vol. 4, no. 2, pp. 1800–1806, Apr. 2019.

[5] T. Matsuda, T. Maki, and T. Sakamaki, "Accurate and efficient seafloor observations with multiple autonomous underwater vehicles: Theory and experiments in a hydrothermal vent field," *IEEE Robot. Automat. Lett.*, vol. 4, no. 3, pp. 2333–2339, Jul. 2019.

[6] M. B. Larsen, "High performance Doppler-inertial navigation-experimental results," in *Proc. Conf. MTS/IEEE Conf. Exhib.*, 2000, pp. 1449–1456.

[7] N. R. Rypkema, "Underwater & out of sight: Towards ubiquity in underwater robotics," Ph.D. dissertation, Massachusetts Inst. Technol., Cambridge, MA, USA, 2019.

[8] N. R. Rypkema and H. Schmidt, "Passive inverted ultra-short baseline (piUSBL) localization: An experimental evaluation of accuracy," in *Proc. IEEE/RSJ Int. Conf. Intell. Robots Syst.*, 2019, pp. 7197–7204.

[9] N. R. Rypkema, E. M. Fischell, and H. Schmidt, "One-way travel-time inverted ultra-short baseline localization for low-cost autonomous underwater vehicles," in *Proc. IEEE Int. Conf. Robot. Automat.*, 2017, pp. 4920–4926.

[10] N. R. Rypkema, E. M. Fischel, and H. Schmidt, "Closed-loop single-beacon passive acoustic navigation for low-cost autonomous underwater vehicles," in *Proc. IEEE/RSJ Int. Conf. Intell. Robots Syst.*, 2018, pp. 641–648.

[11] M. V. Jakuba, J. C. Kinsey, J. W. Partan, and S. E. Webster, "Feasibility of low-power one-way travel-time inverted ultra-short baseline navigation," in *Proc. OCEANS MTS/IEEE Washington*, 2015, pp. 1–10.

[12] E. Fischell, T. Schneider, and H. Schmidt, "Design, implementation, and characterization of precision timing for bistatic acoustic data acquisition," *IEEE J. Ocean. Eng.*, vol. 41, no. 3, pp. 583–591, Jul. 2016.

[13] Y. Wang *et al.*, "Design and experimental results of passive iUSBL for small AUV navigation," *Ocean Eng.*, vol. 248, 2022, Art. no. 110812.

[14] Z. Wang, X. Liu, H. Huang, and Y. Chen, "Development of an autonomous underwater helicopter with high maneuverability," *Appl. Sci.*, vol. 9, no. 19, 2019, Art. no. 4072.

[15] D. Ji, C. Chen, and Y. Chen, "Autonomous underwater helicopters AUV with disc-shaped design for deepwater agility," *Sea Technol.*, vol. 59, 2018, Art. no. 25.

[16] T. C. Yang, "Deconvolved conventional beamforming for a horizontal line array," *IEEE J. Ocean. Eng.*, vol. 43, no. 1, pp. 160–172, Jan. 2018.

[17] T. C. Yang, "Performance analysis of superdirectivity of circular arrays and implications for sonar systems," *IEEE J. Ocean. Eng.*, vol. 44, no. 1, pp. 156–166, Jan. 2019.

[18] M. Y. Feng, S. H. Huang, T. C. Yang, Q. Y. Tu, X. H. Wan, and Y. Q. Wang, "Detection of gas leaks from sea bed using a small circular array," in *Proc. OCEANS-Marseille*, 2019, pp. 1–5.

[19] T. C. Yang, "Deconvolution of decomposed conventional beamforming," *J. Acoustical Soc. Amer.*, vol. 148, no. 2, pp. L195–L201, 2020.